Autophagy

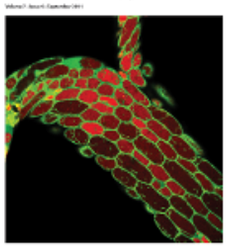

ISSN: 1554-8627 (Print) 1554-8635 (Online) Journal homepage: https://www.tandfonline.com/loi/kaup20

Quercetin induces protective autophagy in gastric cancer cells: Involvement of Akt-mTOR- and hypoxia-induced factor 1α-mediated signaling

Kui Wang, Rui Liu, Jingyi Li, Jiali Mao, Yunlong Lei, Jinhua Wu, Jun Zeng, Tao Zhang, Hong Wu, Lijuan Chen, Canhua Huang & Yuquan Wei

To cite this article: Kui Wang, Rui Liu, Jingyi Li, Jiali Mao, Yunlong Lei, Jinhua Wu, Jun Zeng, Tao Zhang, Hong Wu, Lijuan Chen, Canhua Huang & Yuquan Wei (2011) Quercetin induces protective autophagy in gastric cancer cells: Involvement of Akt-mTOR- and hypoxia-induced factor 1α-mediated signaling, Autophagy, 7:9, 966-978, DOI: 10.4161/auto.7.9.15863

To link to this article: https://doi.org/10.4161/auto.7.9.15863

Autophagy 7:9, 966-978; September 2011; © 2011 Landes Bioscience

Quercetin induces protective autophagy in gastric cancer cells

Involvement of Akt-mTOR- and hypoxia-induced factor 1α-mediated signaling

Kui Wang,[1,†] Rui Liu,[1,†] Jingyi Li,[1,†] Jiali Mao,[1] Yunlong Lei,[1] Jinhua Wu,[1] Jun Zeng,[1] Tao Zhang,[1] Hong Wu,[2] Lijuan Chen,[1] Canhua Huang[1,*] and Yuquan Wei[1]

[1]State Key Laboratory of Biotherapy and Cancer Center; West China Hospital; West China Medical School; Sichuan University; Chengdu, China ;
[2]Department of Hepatobiliary Pancreatic Surgery; West China Hospital; Sichuan University; Chengdu, China

[†]These authors contributed equally to this work.

Key words: quercetin, gastric cancer, autophagy, apoptosis, mTOR, HIF-1α

Abbreviations: mTOR, mammalian target of rapamycin; AVOs, acidic vesicular organelles; GFP, green fluorescent protein; LC3, microtubule-associated protein 1 light chain 3; MTT, 3-(4,5-dimethylthiazol-2-yl)-2,5-diphenyltetrazolium bromide; DMSO, dimethyl sulfoxide; TUNEL, terminal deoxynucleotidyltransferase dUTP nick-end labeling; ELISA, enzyme-linked immunosorbent assay; HIF-1α, hypoxia-induced factor 1α; PHD, prolyl hydroxylase; VHL, von hippel-lindau; siRNA, small interfering RNA; RT-PCR, reverse transcription polymerase chain reaction; PBS, phosphate-buffered saline

Quercetin, a dietary antioxidant present in fruits and vegetables, is a promising cancer chemopreventive agent that inhibits tumor promotion by inducing cell cycle arrest and promoting apoptotic cell death. In this study, we examined the biological activities of quercetin against gastric cancer. Our studies demonstrated that exposure of gastric cancer cells AGS and MKN28 to quercetin resulted in pronounced pro-apoptotic effect through activating the mitochondria pathway. Meanwhile, treatment with quercetin induced appearance of autophagic vacuoles, formation of acidic vesicular organelles (AVOs), conversion of LC3-I to LC3-II, recruitment of LC3-II to the autophagosomes as well as activation of autophagy genes, suggesting that quercetin initiates the autophagic progression in gastric cancer cells. Furthermore, either administration of autophagic inhibitor chloroquine or selective ablation of *atg5* or *beclin 1* using small interfering RNA (siRNA) could augment quercetin-induced apoptotic cell death, suggesting that autophagy plays a protective role against quercetin-induced apoptosis. Moreover, functional studies revealed that quercetin activated autophagy by modulation of Akt-mTOR signaling and hypoxia-induced factor 1α (HIF-1α) signaling. Finally, a xenograft model provided additional evidence for occurrence of quercetin-induced apoptosis and autophagy in vivo. Together, our studies provided new insights regarding the biological and anti-proliferative activities of quercetin against gastric cancer, and may contribute to rational utility and pharmacological study of quercetin in future anti-cancer research.

Introduction

Gastric cancer is the second leading cause of cancer-related deaths, and approximately 760,000 cases of stomach cancer are diagnosed worldwide and more than 24,000 cases are diagnosed in the United States each year.[1] The development of effective therapy for advanced gastric cancer is rather slow and no globally acceptable standard regimen has been established yet.[2]

Quercetin (3,3',4',5,7-pentahydroxyavone), a member of the flavonoids family, is one of the most prominent dietary antioxidants in the human diet,[3,4] and has been approved in clinical trials for tyrosine kinase inhibition.[5] Recently, quercetin has attracted much attention in relation to its anticancer activities in many cancer cell models, including lymphoma, ovary, endometrial, prostate, liver and gastric cancer;[6-9] however, the molecular mechanisms underlying quercetin-mediated cellular responses remain poorly defined.

Autophagy is a highly regulated process involved in turnover of long-lived proteins and whole organelles by lysosomal activity that eliminates supernumerary or damaged organelle.[10-14] The formation of double-membrane autophagosome initiated by PI3 kinase type III-Atg6/Beclin 1 cascade is the main characteristic of autophagy.[15] Expansion of the autophagosome is mediated by two ubiquitin-like conjugation systems: the Atg12-Atg5

*Correspondence to: Canhua Huang; Email: hcanhua@hotmail.com
Submitted: 12/03/10; Revised: 03/21/11; Accepted: 04/13/11
http://dx.doi.org/10.4161/auto.7.9.15863

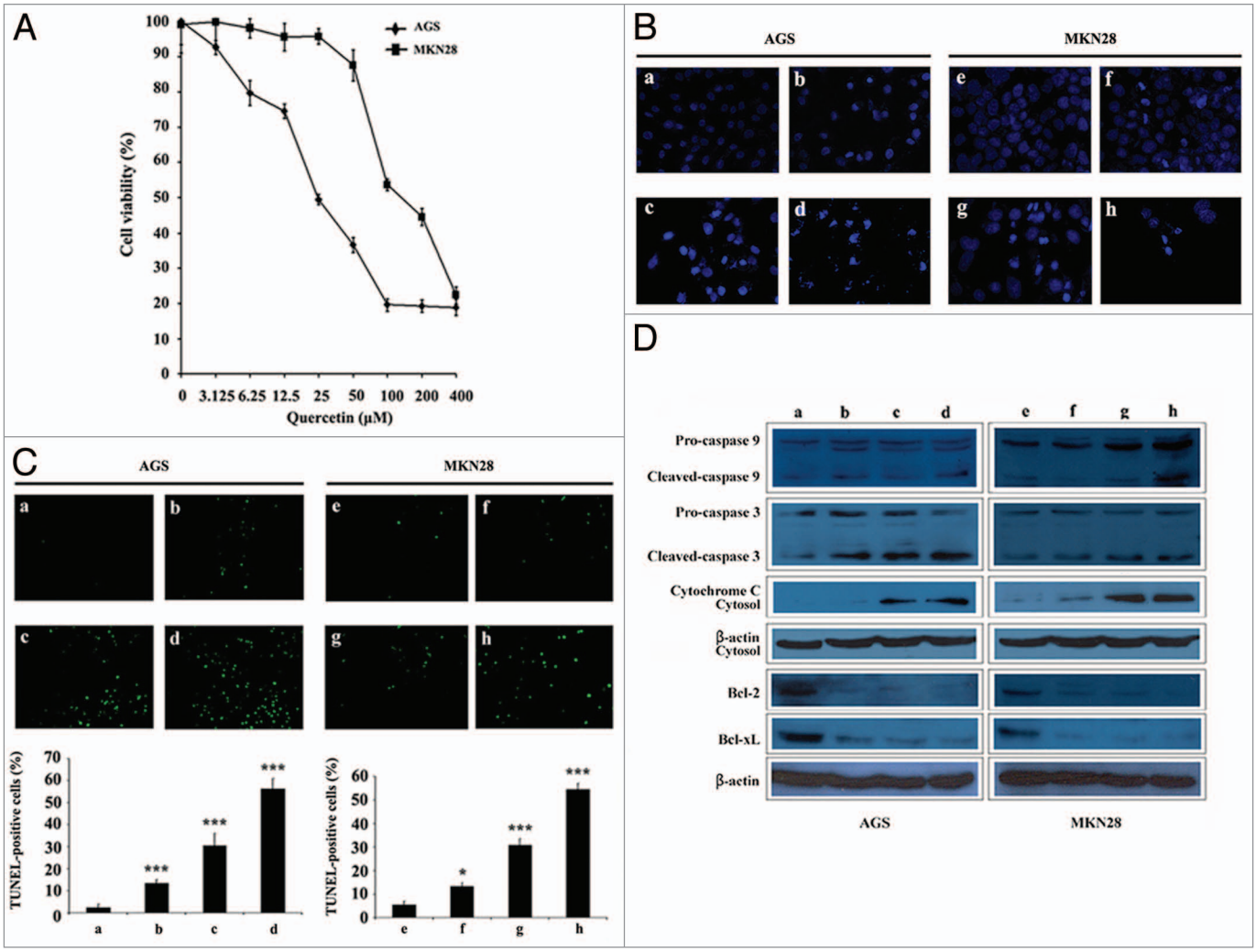

Figure 1. Quercetin induced apoptosis in gastric cancer cells. AGS and MKN28 cells were treated with increasing concentrations of quercetin for 48 h respectively. (A) The cell viability index was measured by MTT assay. (B) Condensed bright blue nuclei by Hoechst staining represented apoptotic cells. (C) TUNEL assay was performed to measure the ratio of apoptotic cells. TUNEL positive cells were counted from at least 100 random fields. (D) Immunoblot analysis of cytosol cytochrome *C*, Bcl-2, Bcl-x_L, caspase 9 and caspase 3 from lysates of AGS and MKN28 cells treated with various concentrations of quercetin for 48 h. (a) DMSO; (b) 10 μM quercetin; (c) 20 μM quercetin; (d) 40 μM quercetin; (e) DMSO; (f) 40 μM quercetin; (g) 80 μM quercetin; (h) 160 μM quercetin. All data were representative of three independent experiments. *$p < 0.05$; **$p < 0.01$; ***$p < 0.001$.

conjugate system and the Atg8/LC3-phosphatidylethanolamine conjugate system.[16] Autophagy signaling can be activated by multiple signaling pathways in response to numerous forms of cellular stress including starvation, hypoxia, radiation or chemical insults.[17] Of them, the classic Akt-mTOR signaling pathway is considered as a typical negative regulator for initiation of the vesicular double-membrane formation,[18] whereas with respect to the positive-regulated upstream signaling, HIF-1α accumulation routinely activates autophagy progression through repressing mTOR1 complex or inducing BNIP3/BNIP3L which can disrupt the interaction of Beclin 1 with Bcl-2/Bcl-x_L.[19,20] The molecular crosstalk between autophagic and apoptotic signaling pathway is complex, and both pathways share several same or interconnected genes that are critical for their respective function.[21] It has been reported that Atg5, which is indispensable in autophagic ubiquitin-like conjugation system, can be cleaved in response to death stimuli and then switches autophagy to apoptosis.[22] In addition, Bcl-2 and Bcl-x_L, 2 well-characterized apoptosis negative regulators, can bind to the BH3 domain of Beclin 1 and retard autophagy progression.[23]

Here we reported a hitherto undescribed cellular response of quercetin-induced protective autophagy in gastric cancer cells, and this process was mediated by modulation of Akt-mTOR signaling and accumulation of HIF-1α. Our studies would provide the groundwork for future studies on the implication of autophagy in quercetin-mediated anticancer activities.

Results

Quercetin induced apoptosis in gastric cancer cells. Cell viability was determined by MTT assay. As shown in **Figure 1A**, treatment with quercetin resulted in growth inhibition of both

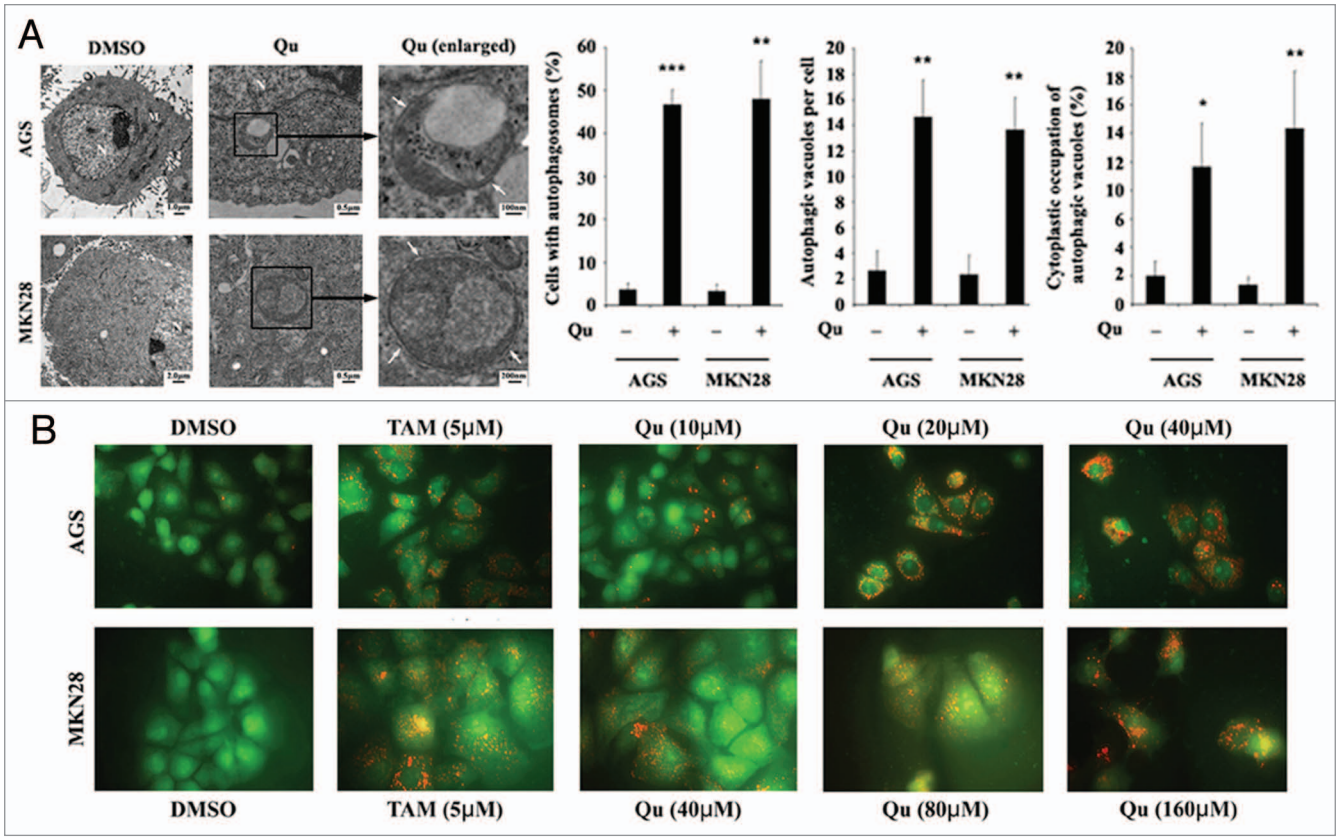

Figure 2. Quercetin induced formation of autophagic vacuoles and AVOs in gastric cancer cells. (A) Representative transmission electron microscopy images of AGS and MKN28 cells treated with DMSO (<0.1%) or quercetin (40 μM for AGS cells and 160 μM for MKN28 cells) for 48 h. The cells with autophagic vacuoles were defined as cells that had five or more autophagic vacuoles. The percentage of the cells with autophagosomes, the average number of autopphagic vacuoles per cell and the cytoplastic occupation of autophagic vacuoles were analyzed from at least 100 random fields. Arrows, autophagic vacuoles. Qu, quercetin; N, nuclear; M, mitochondria. (B) Acridine orange staining of AGS and MKN28 cells treated with DMSO (< 0.1%), 5 μM tamoxifen (positive control) or indicated concentrations of quercetin for 48 h. Qu, quercetin; TAM, tamoxifen. All data were representative of three independent experiments. *p < 0.05; **p < 0.01; ***p < 0.001.

AGS and MKN28 cells in a dose-dependent manner. The IC_{50} values of quercetin against AGS and MKN28 cells were 40 μM and 160 μM, respectively. In addition, we examined apoptotic effect of quercetin in gastric cancer cells using a combination of Hoechst staining, cell death detection ELISA^{Plus} and TUNEL assays. As shown in **Figure 1B**, quercetin induced condensed bright blue apoptotic nuclei in gastric cancer cells in a dose-dependent manner. Consistent with this observation, DNA fragmentation ratio of quercetin-treated groups was predominantly elevated compared with DMSO-control group examined by both cell death detection ELISA^{Plus} and TUNEL assays (**Fig. 1C; Fig. S1A**). To further explore the biological effects of quercetin in vivo, a mouse xenograft model was established. We found that intraperitoneal injections of quercetin resulted in a remarkable reduction of tumor size. As shown in **Figure S1C**, the average tumor size of quercetin-treated mice shrank by ~70% compared with the vehicle-treated control mice. Immunohistochemistry analysis of K_i-67 showed that quercetin inhibited cell proliferation in gastric tumor xenograft (**Fig. S1D**). Consistent with this observation, TUNEL assay revealed that quercetin treatment resulted in massive apoptotic cell death in gastric tumor xenograft (**Fig. S1E**).

Next, we examined whether quercetin-induced cell death was caspase-dependent using immunoblot analysis. As shown in **Figure 1D** (the upper two parts), both cleaved-caspase 9 and cleaved-caspase 3 were accumulated upon quercetin treatment. Moreover, quercetin-induced cell death could be markedly reversed by a pan-caspase inhibitor, Z-VAD-fmk (**Fig. S1B**). Intriguingly, we found that quercetin effectively decreased expression of Bcl-2 and Bcl-x_L as well as induced the leakage of cytochrome *C* from mitochondria (**Fig. 1D**). Our data indicated that quercetin induced the caspase-dependent and mitochondria-mediated apoptotic cell death.

Quercetin induced formation of autophagic vacuoles and AVOs in gastric cancer cells. To better understand the anticancer effect of quercetin, we examined other cellular responses associated with cell death under quercetin treatment. As shown in **Figure S2A**, in contrast to the DMSO-control group, numerous microscopic vacuoles were observed in both AGS and MKN28 cells treated with quercetin. As formation of double-membrane autophagic vacuoles is a main feature of autophagy,[16] we have a particular interest in examining the ultrastructural details of the vacuoles using transmission electron microscropy. As indicated in **Figure 2A**, various membrane-associated vacuoles appeared

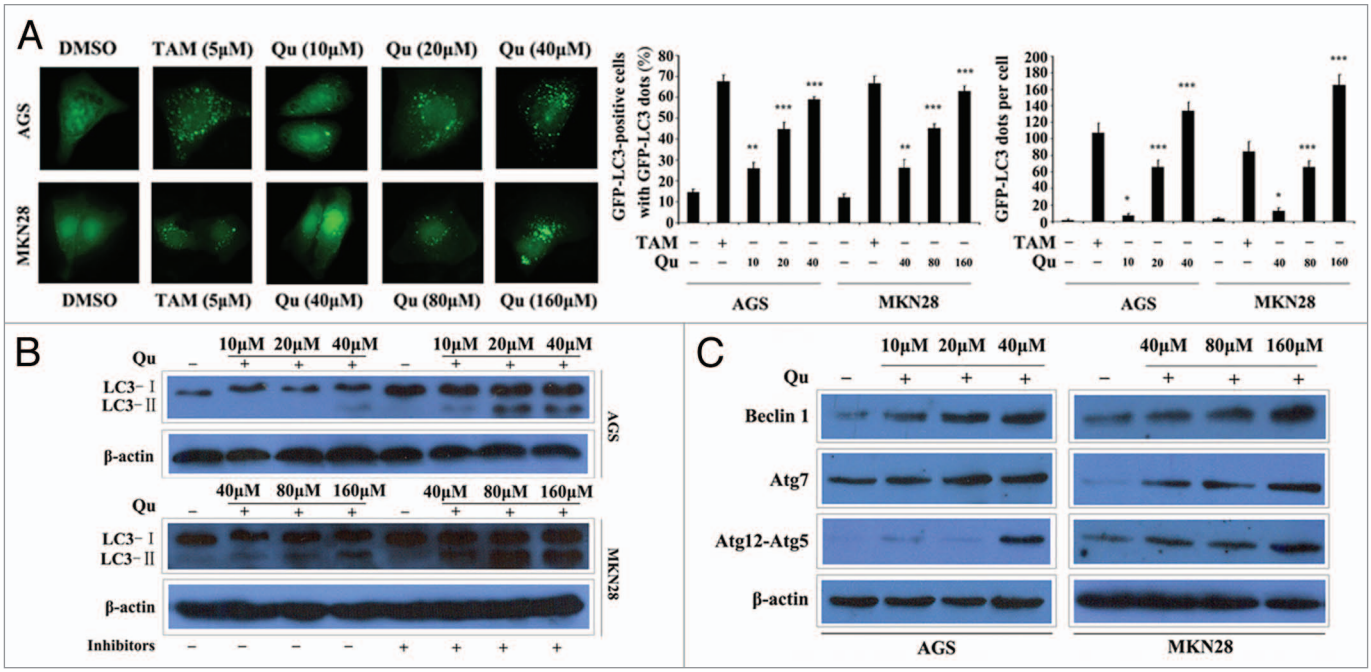

Figure 3. Quercetin induced LC3 turnover and activated autophagy-related genes in gastric cancer cells. (A) AGS and MKN28 cells were transiently transfected with pEGFP-LC3 plasmid and treated with DMSO (<0.1%), 5 μM tamoxifen (positive control) or indicated concentrations of quercetin for 48 h. GFP-LC3 positive cells were defined as that cells have five or more GFP-LC3 punctate dots. The percentage of GFP-LC3 positive cells with GFP-LC3 dots and the average number of GFP-LC3 dots per cell were assessed from 100 random fields. (B) Immunoblot analysis of LC3 expression from lysates of AGS and MKN28 cells treated with various concentrations of quercetin for 48 h in the absence or presence of lysosomal inhibitors (E64d and pepstatin each at 10 μg/ml). (C) Immunoblot analysis of Beclin 1, Atg7 and Atg12-Atg5 conjugate expression from lysates of AGS and MKN28 cells treated with various concentrations of quercetin for 48 h. β-actin was used as the internal control. Qu, quercetin; TAM, tamoxifen. All data were representative of three independent experiments. *p < 0.05; **p < 0.01; ***p < 0.001.

in the cytoplasm of both AGS and MKN28 cells treated with quercetin. To further characterize the membrane-associated vacuoles, acridine orange staining was used to analyze the formation of acidic vesicular organelles (AVOs), a main feature of autophagy.[24,25] As shown in **Figure 2B**, similar to tamoxifen (a commonly used autophagy inducer), quercetin induced pronounced formation of orange AVOs in a dose-dependent manner in gastric cancer cells, while the DMSO-treated cells primarily exhibit green fluorescence, indicating the lack of AVOs.

Quercetin induced LC3 turnover and activated autophagy-related genes in gastric cancer cells. The lipidated form of LC3 transforming from LC3-I to LC3-II has been considered to be an autophagosomal marker due to its localization and aggregation on autophagosomes.[26,27] To find out whether LC3 was involved in quercetin-induced autophagy, pEGFP-LC3 plasmid was transiently transfected into both AGS and MKN28 cells. As indicated in **Figure 3A**, the DMSO-treated control cells revealed diffused and weak LC3 punctate dots, whereas the tamoxifen (positive control) or quercetin-treated cells exhibited a cornucopia of green LC3 punctate dots in the cytoplasm. Both the percentage of cells with GFP-LC3 dots and average number of GFP-LC3 dots per cell were increased in a dose-dependent manner. Moreover, to examine whether quercetin treatment induced processing of full-length LC3-I (18 kDa) to LC3-II (16 kDa), immunoblot analysis was performed.[28] As shown in **Figure 3B**, LC3-II was accumulated in quercetin-treated AGS and MKN28 cells, and the accumulation was more pronounced with the dose of quercetin increased. Furthermore, in vivo studies provided additional data showing that expression of LC3 and accumulation of LC3-II were markedly increased in gastric tumor xenograft in response to quercetin treatment (**Fig. S2B and C**).

During autophagy, a series of autophagy genes associated with formation of autophagosome are largely activated.[29] The isolation membrane is formed as a result of the activation of the Beclin 1-Vps34 complex, and subsequently elongated with the help of the ubiquitin-conjugation system.[21] *Atg7*, a key autophagy gene, encodes a protein resembling E ubiquitin-activating enzyme that contributes to both of the ubiquitin-like pathways essential to form autophagic vascuoles.[30] Atg12 is activated by Atg7, then transferred to Atg10 and finally covalently attached to Atg5 to be Atg12-Atg5 conjugate which localizes to autophagosome precursors.[21] To examine whether autophagy genes were synergistically activated corresponding to quercetin-induced autophagy, RT-PCR and immunoblot analyses were utilized to measure expression of Beclin 1, Atg7 and Atg12-Atg5 conjugate at mRNA and protein levels, respectively. As a result, we found that quercetin upregulated expression of all these autophagy-related genes in a dose-dependent manner (**Fig. 3C; Fig. S2D**).

Inhibition of autophagy enhanced quercetin-induced apoptosis in gastric cancer cells. Accumulating evidence suggested a paradoxical role of autophagy in control of cell death and survival under various stimulus conditions.[31-36] To determine the

biological role of autophagy in quercetin-mediated apoptotic cell death, the autophagy inhibitor chloroquine was utilized to disrupt lysosomal function and prevent completion of autophagy. To this end, cells were treated with chloroquine, quercetin alone or in combination. Our study showed that chloroquine enhanced quercetin-induced suppression of gastric cancer cell growth (**Fig. 4A**). In line with this observation, quercetin-induced apoptotic cell death was augmented in the presence of chloroquine, which was demonstrated by both cell death detection ELISA^{Plus} and TUNEL assays to detect the DNA fragmentation (**Fig. 4B and C**).

Considering that chloroquine might have effects on lysosomes that are independent of autophagy, an alternate approach was applied to block the formation of autophagosomes by knocking down expression of key autophagy genes using either *atg5* or *beclin 1* specific small interfering RNA. The expression level of either Atg5 or Beclin 1 was markedly reduced in gastric cancer cells transiently transfected with the *atg5*- or *beclin* 1-targeted siRNA respectively, compared with nonspecific siRNA-transfected cells (**Fig. S3**). Our data demonstrated that silencing expression of either *atg5* or *beclin 1* could markedly enhance quercetin-induced inhibition of gastric cancer cell growth and promote the apoptotic cell death (**Fig. 5A–C**). Collectively, our studies suggested that quercetin-induced autophagy plays a protective role against apoptotic cell death in gastric cancer cells.

Quercetin inhibited the Akt-mTOR signaling pathway in gastric cancer cells. The Akt-mTOR signaling is considered a key negative regulator of autophagy;[13] therefore, we examined if phosphorylation of both Akt and mTOR was involved in quercetin-induced autophagy in gastric cancer cells. As shown in **Figure 6A**, quercetin treatment resulted in a notable inhibition of both Akt (S473) and mTOR (S2448) phosphorylation in AGS and MKN28 cells. In addition, quercetin-mediated dephosphorylation of Akt and mTOR was more pronounced with the dose of quercetin increased. As mTOR has been reported to control protein synthesis through phosphorylation of downstream p70 S6K and 4E-BP1,[37] we have a particular interest in examining the phosphorylation status of both p70 S6K (S424/T421) and 4E-BP1 (S65/T70) by immunoblot analysis. As shown in **Figure 6B**, quercetin treatment dephosphorylated both p70 S6K (S424/T421) and 4E-BP1 (S65/T70) in a dose-dependent manner.

HIF-1α accumulation mediated quercetin-induced autophagy in gastric cancer cells. Next, we examined whether HIF-1α, an upstream regulator of autophagy, was involved in quercetin-induced autophagy.[37] Immunoblot analysis revealed that quercetin induced upregulation of HIF-1α expression in a dose-dependent manner in both AGS and MKN28 cells (**Fig. 7A**). In addition, both immunohistochemistry and immunoblot analyses revealed that quercetin treatment resulted in HIF-1α accumulation in tumor xenograft (**Fig. S4A and B**). To better understand the functional role of HIF-1α in quercetin-induced autophagy, the HIF-1α inhibitor YC-1 was applied to repress HIF-1α expression. In a pilot study, we found that 5 μM YC-1 was sufficient to reverse quercetin-induced HIF-1α accumulation (**Fig. S4C**). Intriguingly, in the presence of YC-1, both the percentage of cells with GFP-LC3 dots and average number of GFP-LC3 dots per cell were decreased in either AGS or MKN28 cells under quercetin treatment (**Fig. 7B**). In addition, immunoblot analysis revealed that addition of YC-1 markedly inhibited the quercetin-induced LC3 turnover as well as expression of Beclin 1, Atg7 and Atg12-Atg5 conjugate (**Fig. 7C and D**).

Further, we investigated the role of HIF-1α in quercetin-induced autophagy. We found that inhibition of HIF-1α accumulation by YC-1 could restore the mTOR signaling, as shown by immunoblot analysis of phosphorylation of mTOR (S2448), p70 S6K (S424/T421) and 4E-BP1 (S65/T70) (**Fig. 7E; Fig. S4D**). In addition to mTOR signaling, it has been reported that HIF-1α accumulation could activate autophagy progression by inducing expression of BNIP3/BNIP3L which disrupts the interaction of Beclin 1 with Bcl-2/Bcl-x_L.[19,20] In our study, we found that quercetin stimulated accumulation of both BNIP3 and BNIP3L, while this effect could be blocked by YC-1 administration (**Fig. 7F; Fig. S4E**). Moreover, to determine the biological effect of quercetin on Beclin 1/Bcl-2 (Bcl-x_L) complex, co-immunoprecipitation was performed to monitor the interaction of Beclin 1 with Bcl-2/Bcl-x_L. As indicated in **Figure 7G**, under basal conditions Beclin 1 and Bcl-2/Bcl-x_L co-immunoprecipitated with each other in AGS and MKN28 cells whereas this interaction markedly decreased in quercetin-treated cells. Together, our studies supported a notion that accumulation of HIF-1α played an important role in quercetin-induced autophagy in gastric cancer cells.

Discussion

Quercetin, an extensive class of polyphenolic flavonoid compounds almost ubiquitous in plants and plant food sources, has been studied as a promising chemoprevention agent in a variety of cancer models.[38] Consistent with previous reports, our study showed that quercetin inhibited proliferation and induced apoptosis in gastric cancer cells.[9]

Autophagy is an evolutionary conserved, dynamic and lysosome-mediated process that involves the sequestration and delivery of cytoplasmic material to the lysosome where it is degraded and recycled.[39,40] Accumulating anticancer agents have been documented to trigger the cellular autophagic process, but the role that autophagy plays in cancer chemotherapy is still controversial. Certain anticancer agents i.e., polyoxomolybdates-, platonin- or phenethyl isothiocyanate could induce autophagic cell death to enhance chemotherapeutic efficacy,[41-43] while others, i.e., suberoylanilide hydroxamic acid, arginine deiminase or timosaponin A-III mediated protective autophagy that antagonized apoptotic cell death.[31-33] In this study, we demonstrated that quercetin triggered autophagy in human gastric cancer cells both in vitro and in vivo. Further functional analysis showed that inhibition of autophagy markedly increased quercetin-induced apoptotic cell death, suggesting that quercetin-induced autophagy plays a protective role in gastric cancer cells.

The Akt-mTOR signaling pathway is the major negative signaling pathway against autophagy and previous studies indicated that quercetin repressed phosphorylation of Akt in salivary adenoid cystic carcinoma and prostate adenocarcinoma.[13,44,45] In the

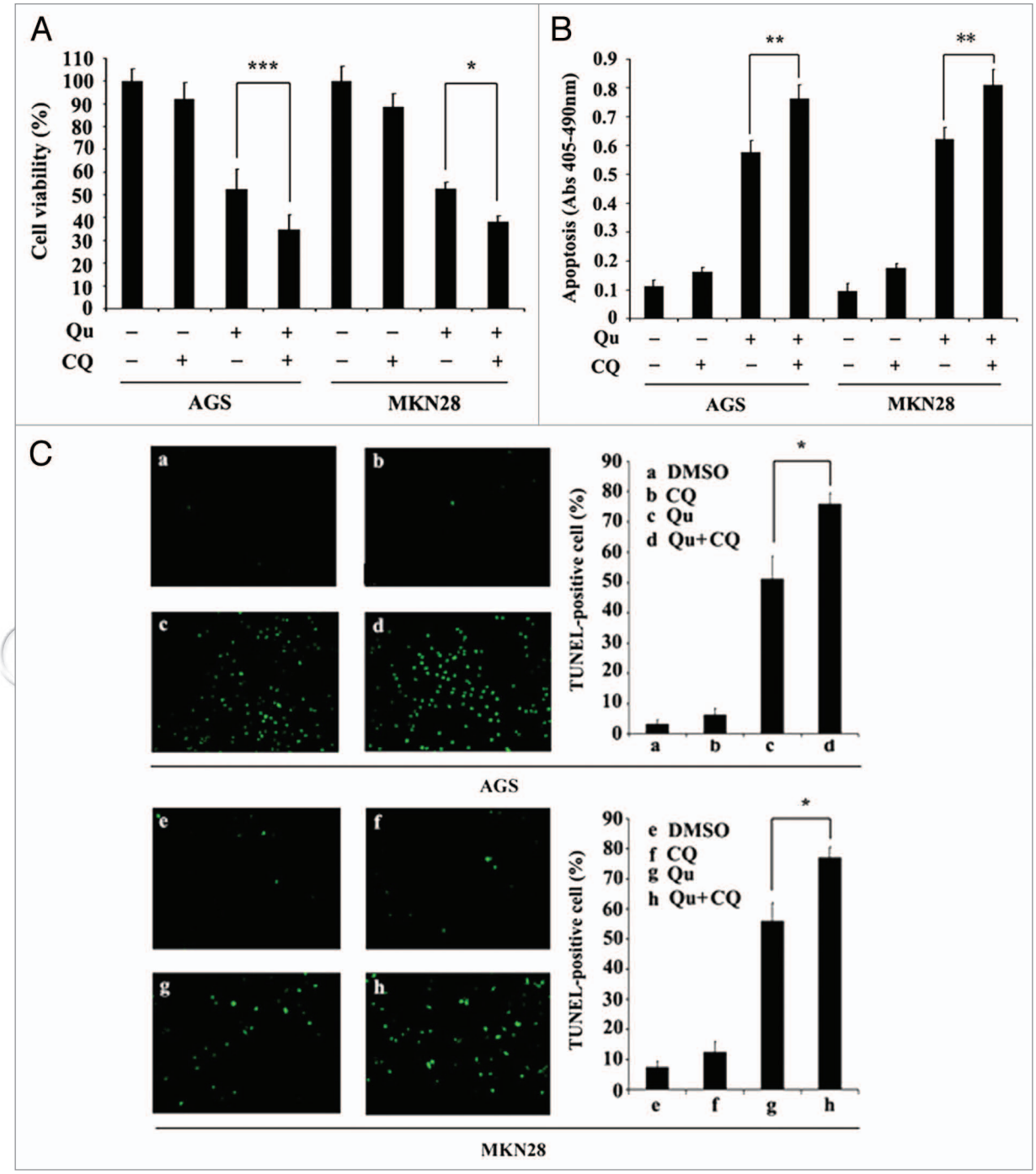

Figure 4. Inhibition of autophagy by chloroquine administration enhanced quercetin-induced apoptosis in gastric cancer cells. (A) Cell viability was assessed by MTT assay in AGS and MKN28 cells treated with DMSO (<0.1%) and quercetin (40 μM for AGS cells and 160 μM for MKN28 cells) in the absence or presence of 20 μM chloroquine for 48 h. (B) Apoptotic ratios were assessed by cell death detection ELISA^{Plus} assay in AGS and MKN28 cells treated with DMSO (<0.1%) and quercetin (40 μM for AGS cells and 160 μM for MKN28 cells) in the absence or presence of 20 μM chloroquine for 48 h. (C) TUNEL assay was performed to measure apoptotic ratios in AGS and MKN28 cells. (a) DMSO control (<0.1%); (b) 20 μM chloroquine; (c) 40 μM quercetin; (d) combination of 40 μM quercetin with 20 μM chloroquine; (e) DMSO control (<0.1%); (f) 20 μM chloroquine; (g) 160 μM quercetin; (h) combination of 160 μM quercetin with 20 μM chloroquine. Qu, quercetin. CQ, chloroquine. All data were representative of three independent experiments. *$p < 0.05$; **$p < 0.01$; ***$p < 0.001$.

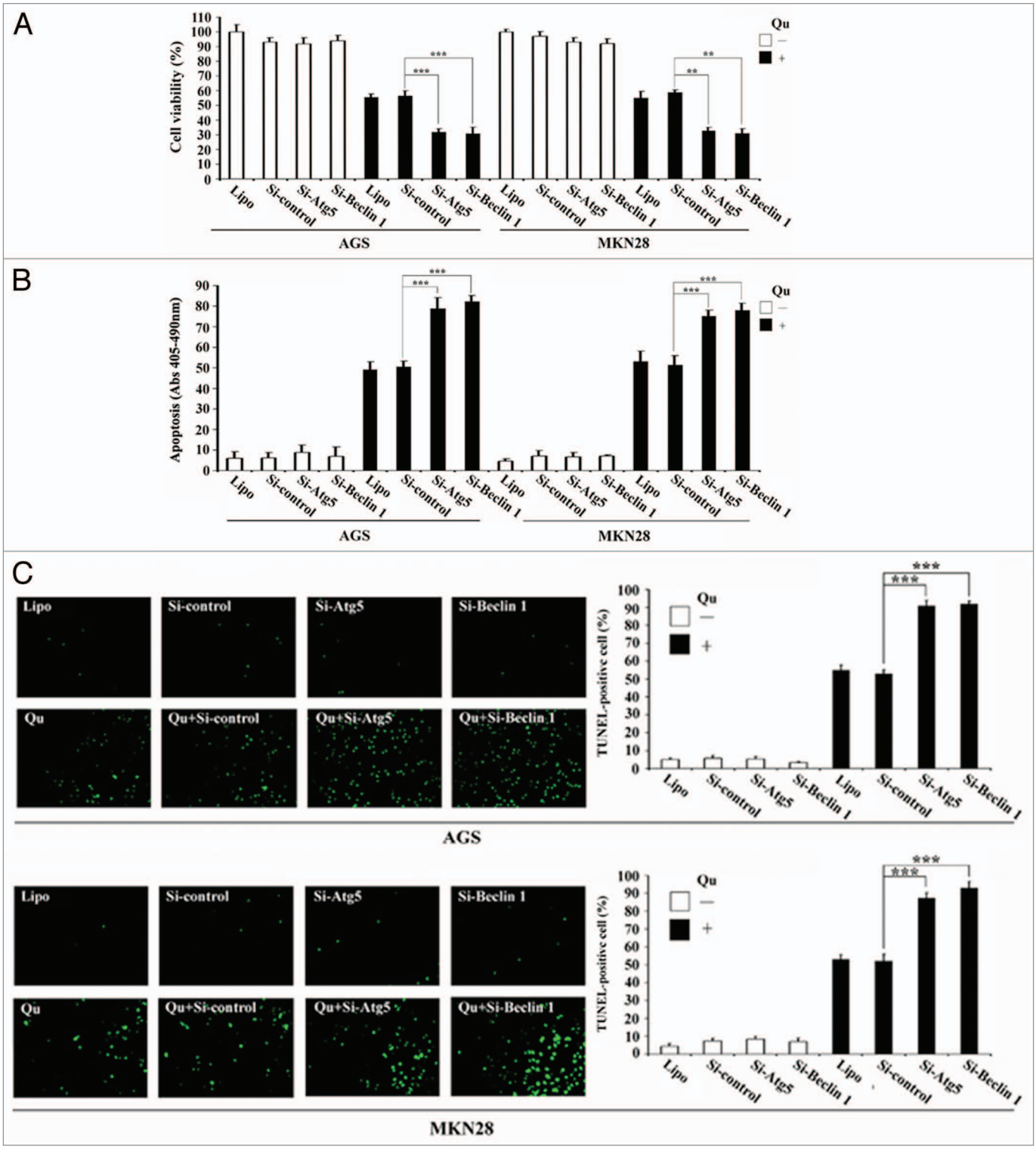

Figure 5. Inhibition of autophagy by *atg5* or *beclin 1* siRNA enhanced quercetin-induced apoptosis in gastric cancer cells. Cells were transfected with control siRNA, *atg5*- or *beclin 1*-targeted siRNA in the absence or presence of quercetin (40 μM for AGS cells and 160 μM for MKN28 cells) for 48 h. (A) Cell viability was assessed by MTT assay in AGS and MKN28 cells. (B) Apoptosis ratios were assessed by cell death detection ELISA^{Plus} assay in AGS and MKN28 cells. (C) TUNEL assay was performed to measure apoptotic ratios in AGS and MKN28 cells. TUNEL positive cells were counted from at least 100 random fields. Qu, quercetin; Lipo, Lipofectamine 2000. All data were representative of three independent experiments. *$p < 0.05$; **$p < 0.01$; ***$p < 0.001$.

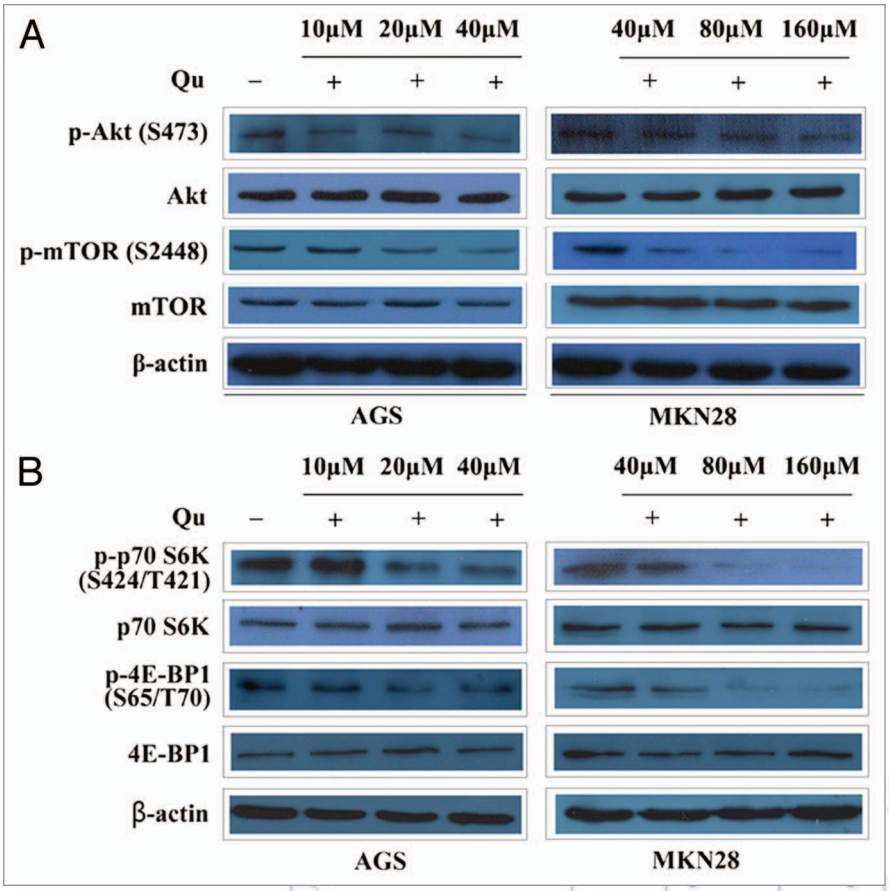

Figure 6. Quercetin suppressed the Akt-mTOR signaling pathway in gastric cancer cells. (A) Immunoblot analysis of phospho-Akt (S473), total Akt, phospho-mTOR (S2448) and total mTOR from lysates of AGS and MKN28 cells treated with various concentrations of quercetin for 48 h. (B) Immunoblot analysis of phospho-p70 S6K (S424/T421), total p70 S6K, phospho-4E-BP1 (S65/T70) and total 4E-BP1 from lysates of AGS and MKN28 cells treated with various concentrations of quercetin for 48 h. β-actin was used as the internal control. Qu, quercetin. All data were representative of three independent experiments.

present study, our data demonstrated that quercetin dephosphorylated Akt and mTOR as well as p70 S6K and 4E-BP1 (two best characterized targets of mTOR1 complex) in gastric cancer cells, which underscored the functional importance of the involvement of Akt-mTOR signaling in quercetin-mediated protective autophagy in gastric cancer cells.

HIF-1α activates the transcription of genes that are involved in crucial aspects of cancer biology, including angiogenesis, cell survival, glucose metabolism and invasion.[46] Prolyl hydroxylase (PHD) mediates the recognition of von Hippel-Lindau protein (VHL) which determines the ubiquitination of HIF-1α in 26S proteasome degradation system.[47] Previous studies reveal that in human lens epithelial cells, prostate adenocarcinoma cells, colon carcinoma cells and uterine cervix cancer cells, quercetin can stabilize HIF-1α through chelation of intracellular ferrous ion which is one of the cofactors of PHD, relying on the special natural chemical constitution of quercetin that contains several hydroxy and oxo groups which specifically chelated with ferrous ion.[48-51] Consistent with these reports, our present study revealed a remarkable HIF-1α accumulation in gastric cancer cells as well as gastric tumor xenograft model in response to quercetin treatment. Our data supported the notion that upregulation of HIF-1α expression was a common cellular response in cancer cells upon quercetin treatment.

Increasing evidence suggests that HIF-1α plays an important role in autophagy progression by either repressing mTOR complex or enhancing BNIP3/BNIP3L that recovers Beclin 1 pro-autophagic function.[19,20,37,52] In our current study, our data demonstrated that quercetin-induced LC3 turnover as well as Beclin 1, Atg7 and Atg12-Atg5 conjugate accumulation, could be reversed by HIF-1α inhibitor YC-1, indicating that HIF-1α accumulation was crucial for quercetin-induced autophagy. Intriguingly, the dephosphorylation of mTOR and its downstream molecules p70 S6K and 4E-BP1 by quercetin was demonstrated to be reversed by YC-1, suggesting that quercetin-induced mTOR inactivation was mediated by HIF-1α. In addition to mTOR signaling, BNIP3/BNIP3L is a known HIF-1α target that has been implicated in autophagy by disrupting the interaction between Beclin 1 and Bcl-2/Bcl-x_L.[53] The results indicated that BNIP3 and BNIP3L were both activated upon quercetin treatment, which could be inhibited by YC-1. Further data indicated that the interaction of Beclin 1 with Bcl-2/Bcl-x_L in gastric cancer cells was dissociated under quercetin treatment. Taken together, our data demonstrated that HIF-1α was a pivotal factor in quercetin-induced autophagy, by repressing mTOR1 signaling and inducing expression of BNIP3/BNIP3L which disrupted the interaction of Beclin 1 with Bcl-2/Bcl-x_L.

In conclusion, our current study revealed a hitherto undescribed cellular response showing that quercetin induced autophagy antagonizing apoptotic cell death in gastric cancer cells. In addition, we also demonstrated involvement of Akt-mTOR and HIF-1α signaling in quercetin-induced autophagic progression (**Fig. 8**). Information provided in this report would be valuable for further studies and rational utility of quercetin for therapeutic treatment with various cancer diseases.

Materials and Methods

Cell culture and reagents. Human gastric adenocarcinoma cell line AGS (ATCC, CRL-1739) and MKN28 (JCRB, 0253) were cultured in RPMI1640 medium (ATCC, 30-2001) supplemented with 10% fetal bovine serum (ATCC, 30-2020), 100 U/ml penicillin, 100 μg/ml streptomycin (Sigma, P0781) at 37°C in a humidified atmosphere containing 5% CO_2.

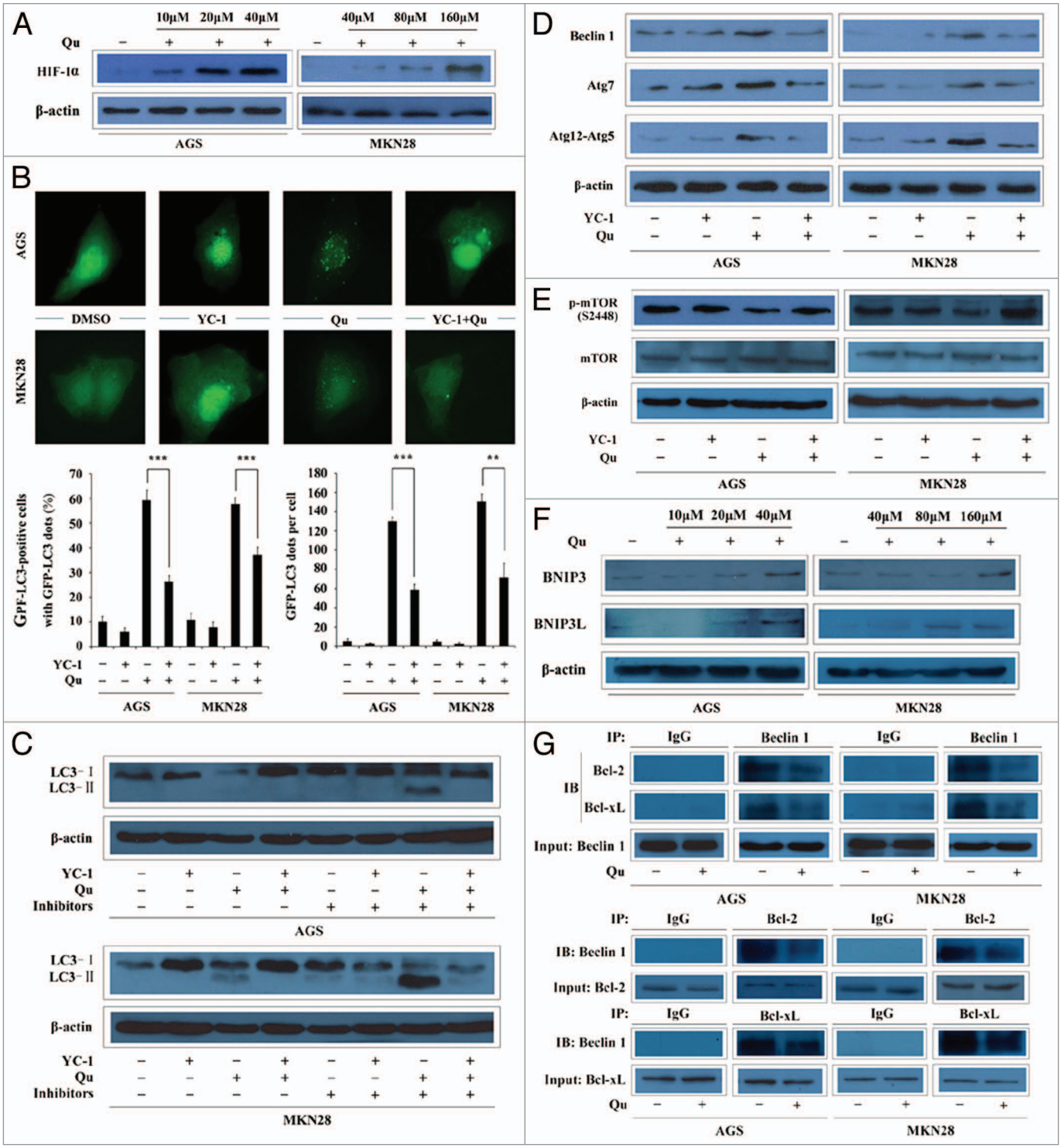

Figure 7. For figure legend, see page 975.

Reagents used were as follows: Quercetin (Sigma, Q4951), MTT (Sigma, M2128), chloroquine (Sigma, C6628), tamoxifen (Sigma, T5648), Hoechst 33342 (Sigma, B2261), acridine orange (Sigma, A6014), DMSO (Sigma, D2650), pepstatin A (Sigma, P4265), E64d (Sigma, E8640), YC-1 (Cayman Chemical, 81560), Z-VAD-fmk (Sigma, V116). Quercetin, tamoxifen, pepstatin A and E64d were dissolved in DMSO, while MTT, chloroquine, Hoechst 33342, acridine orange, YC-1 were dissolved in phosphate-buffered saline (PBS).

Antibodies were obtained from the following sources: Beclin 1 (Santa Cruz, sc-11427), LC3 (Abcam, ab58610), Atg5 (Abcam, ab78073), Atg7 (Abcam, ab53255), β-actin (Santa

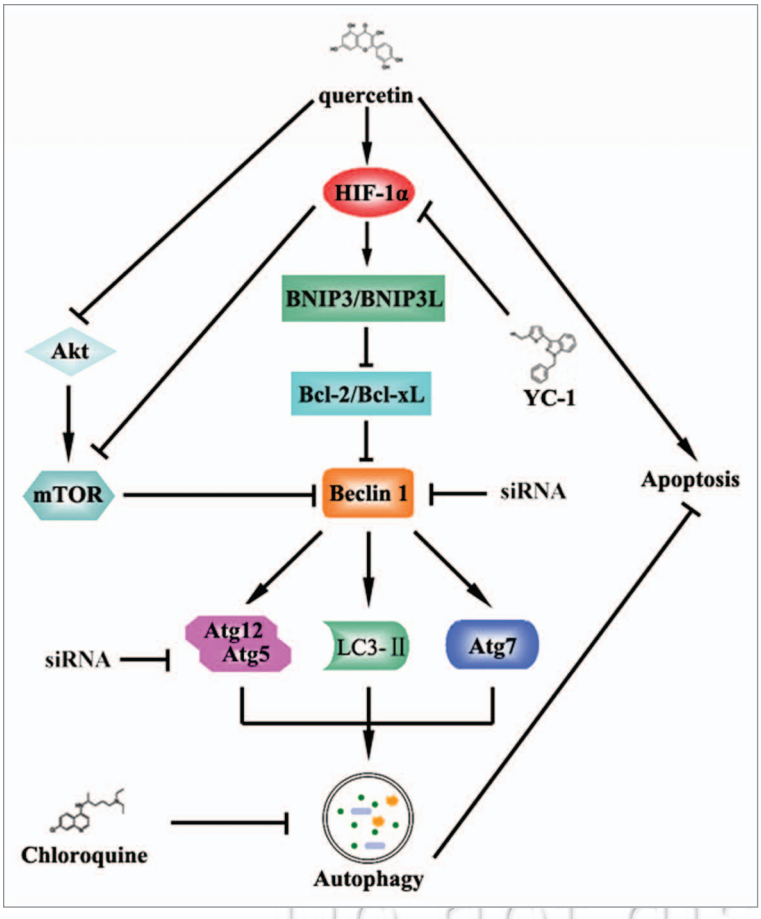

Figure 8. Schematic model illustrating the potential pathway associated with quercetin-induced autophagy. Quercetin triggers accumulation of HIF-1α, which represses mTOR signaling and induces expression of BNIP3/BNIP3L to disrupt the Beclin 1/Bcl-2(Bcl-x_L) complex, leading to activation of Atg7, Atg12-Atg5 conjugate and LC3 turnover. Disruption of the autophagy process by using either lysosomal inhibitor chloroquine or *beclin1/atg 5*-targeted siRNA could markedly enhance quercetin-induced apoptosis in gastric cancer cells.

Cruz, sc-1616), Akt (Cell Signaling, 4685), phospho-Akt (Cell Signaling, 4051), mTOR (Milipore, 04-385), phospho-mTOR (Milipore, 09-213), HIF-1α (Santa Cruz, sc-10790), cytochrome *C* (Santa Cruz, sc-81752), Bcl-2 (Santa Cruz, sc-492), Bcl-x_L (Santa Cruz, sc-7195), caspase 3 (Milipore, MAB4703), caspase 9 (Milipore, 05-572), p70 S6K (Santa Cruz, sc-9027), phospho-p70 S6K (Santa Cruz, sc-7984-R), 4E-BP1 (Santa Cruz, sc-6025), phospho-4E-BP1 (Santa Cruz, sc-12884), BNIP3 (Santa Cruz, sc-56167), BNIP3L (Santa Cruz, sc-28240), K_i-67 (Abcam, ab66155), horseradish peroxidase (HRP)-conjugated anti-rabbit secondary antibody (Santa Cruz, sc-2004), horseradish peroxidase (HRP)-conjugated anti-mouse secondary antibody (Santa Cruz, sc-2005).

Cell viability assay. Cells were seeded in 96-well culture plates and treated for 48 h. Subsequently the cell viabilities were evaluated by MTT assays. The absorbance was measured at 490 nm test wavelength and 570 nm reference wavelength with enzyme-linked immunosorbent assay multi-well spectrophotometer (MDC, Sunnyrale, CA).

Hoechst 33342 staining assay. Cells were cultured in 6-well plates with different concentrations of quercetin for 48 h. After depletion of medium, cells were washed with PBS once and fixed by 4% paraformaldehyde for 15 min. Subsequently, Hoechst 33342 diluted by PBS was added into each well for 10 min, followed by washing with PBS for 10 min twice, the blue stained nuclei were observed by fluorescence microscopy (Olympus Optical Co., Hamburg, Germany) immediately.

Cell death detection ELISA^{Plus} assay. Cell death detection ELISA^{Plus} assay (Roche, 11774425001) was applied to measure apoptosis by quantification of histone-complexed DNA fragments (mono- and oligonucleaosomes) according to the manufacturer's instructions.[54] Absorbance was determined at 405 nm test wavelength and 490 nm reference wavelength using enzyme-linked immunosorbent assay multi-well spectrophotometer (MDC, Sunnyrale, CA).

TUNEL assay. TUNEL staining was performed using the DeadEnd™ Fluorometric TUNEL system according to the manufacturer's instructions (Promega, G3250). Cells were then observed under a fluorescence microscope (Olympus Optical Co., Hamburg, Germany), and a nucleus with bright green fluorescence staining was recorded as a TUNEL-positive event.

Figure 7 (See opposite page). Quercetin-induced autophagy was mediated by HIF-1α accumulation in gastric cancer cells. (A) Immunoblot analysis of HIF-1α from lysates of AGS and MKN28 cells treated with various concentrations of quercetin for 48 h. (B) AGS and MKN28 cells were transiently transfected with pEGFP-LC3 plasmid and treated with DMSO (<0.1%), YC-1 (5 μM), quercetin (40 μM for AGS cells and 160 μM for MKN28 cells) or in combination of quercetin with YC-1 for 48 h. GFP-LC3 positive cells were defined as cells that have five or more GFP-LC3 punctate dots. The percentage of GFP-LC3 positive cells with GFP-LC3 dots and the average number of GFP-LC3 dots per cell were assessed from 100 random fields. (C) Immunoblot analysis of LC3 expression from lysates of AGS and MKN28 cells treated with DMSO (<0.1%), YC-1 (5 μM), quercetin (40 μM for AGS cells and 160 μM for MKN28 cells) or in combination of quercetin with YC-1 for 48 h in the absence or presence of lysosomal inhibitors (E64d and pepstatin each at 10 μg/ml). (D) Immunoblot analysis of Beclin 1, Atg7 and Atg12-Atg5 conjugate expression from lysates of AGS and MKN28 cells treated with DMSO (<0.1%), YC-1 (5 μM), quercetin (40 μM for AGS cells and 160 μM for MKN28 cells) or in combination of quercetin with YC-1 for 48 h. (E) Immunoblot analysis of phospho-mTOR (S2448) and total mTOR from lysates of AGS and MKN28 cells treated with DMSO (<0.1%), YC-1 (5 μM), quercetin (40 μM for AGS cells and 160 μM for MKN28 cells) or in combination of quercetin with YC-1 for 48 h. (F) Immunoblot analysis of BNIP3 and BNIP3L from lysates of AGS and MKN28 cells treated with various concentrations of quercetin for 48 h. (G) Co-immunoprecipitation analysis of Beclin 1 and Bcl-2/Bcl-x_L from lysates of AGS and MKN28 cells treated with DMSO (<0.1%) or quercetin (40 μM for AGS cells and 160 μM for MKN28 cells). β-actin was used as the internal control. Qu, quercetin; IP, immunoprecipitation; IB, immunoblot. All data were representative of three independent experiments. *$p < 0.05$; **$p < 0.01$; ***$p < 0.001$.

Immunoblot. Both adherent and floating cells were collected. Total cell protein was extracted in RIPA buffer (50 mM Tris, 1.0 mM EDTA, 150 mM NaCl, 0.1% SDS, 1% Triton X-100, 1% sodium deoxycholate, 1 mM PMSF). Isolation of mitochondrial and cytosolic protein was performed using the Mitochondria/cytosol Fractionation Kit (Milipore, MIT1000) according to the manufacturer's instructions. The concentrations of protein were quantified by the DC protein assay kit (Bio-Rad, 500-0121). Cellular lysates were resolved on SDS-PAGE and electrophoretically transferred to polyvinylidene difluoride membranes. Membranes were blocked with a buffer containing Tris (10 mmol/L, pH 7.4), NaCl (150 mmol/L), Tween 20 (0.1%) and bovine serum albumin (5%) and then incubated with the primary antibodies at 4°C overnight. Subsequently, membranes were washed and treated with appropriate secondary antibodies conjugated to horseradish peroxidase for 2 h. The immunoreactivities were visualized by enhanced chemiluminescence reagents (Millipore, WBKLS0500). β-actin was used as an internal control.

Transmission electron microscopy. Cells were fixed in 0.1% glutaraldehyde in 0.1 M sodium cacodylate for 2 h, postfixed with 1% OsO_4 for 1.5 h, washed and finally stained for 1 h in 3% aqueous uranyl acetate. The samples were then rinsed with water again, dehydrated with graded alcohol (50%, 75% and 95–100% alcohol) and embedded in Epon-Araldite resin (Canemco, 034). Ultrathin sections were cut on a Reichert Ultramicrotome, counterstained with 0.3% lead citrate and examined on a Philips EM420 transmission electron microscope. The cells with autophagic vacuoles were defined as cells that had 5 or more autophagic vacuoles.[55] Values for the area occupied by autophagic vacuoles and the cytoplasm were obtained with Image Pro Plus version 3.[56]

Detection of acidic vesicular organelles (AVOs). Cells were plated on coverslips in 6-well plates and allowed to attach by overnight incubation. Following treatment with DMSO (control), tamoxifen or quercetin, cells were stained with 1 μg/mL acridine orange in PBS for 15 min, washed with PBS and examined under fluorescence microscope (Olympus Optical Co., Hamburg, Germany).

GFP-LC3 transient transfection. Cells were transfected with pEGFP-LC3 plasmid using Lipofectamine 2000 reagent (Invitrogen, 11668027) according to the manufacturer's protocol and were maintained on coverslips in 6-well plates. After transfection for 48 h, cells were treated with different concentrations of quercetin for 48 h. Subsequently, cells were washed with PBS twice and fixed by 4% paraformaldehyde for 15 min. The coverslides with cells were infiltrated with 60% glycerol on the microscope slides, and then the cellular localization pattern of GFP-LC3 protein was photographed using a fluorescence microscopy (Olympus Optical Co., Hamburg, Germany). The percentage of GFP-LC3-positive cells with GFP-LC3 punctate dots was determined from 3 independent experiments. The cells with more than 5 GFP-LC3 punctate dots were counted under blinded conditions. A minimum of 100 total cells were counted at different random fields on each coverslide.

Semiquantitative RT-PCR. Total RNA was isolated using TRIzol reagent (Invitrogen, 15596-026) according to the manufacturer's instructions. First strand cDNA was reverse transcribed from 1 μg of total RNA in a final volume of 20 μl using reverse transcriptase and random hexamers from RevertAid™ First Strand cDNA Synthesis Kit (Fermentas, K1622) according to the manufacturer's instructions. Primers were designed using Primer Premier 5 software. The primers sequence and the expected length of PCR products were as follows: *beclin 1,* sense 5'-CGT GGA ATG GAA TGA GAT-3' and antisense 5'-GGT CAA ACT TGT TGT CCC-3' (209 bp); *atg7*, sense 5'-TTT GCT ATC CTG CCC TCT-3' and antisense 5'-TGC CTC CTT TCT GGT TCT-3' (492 bp); *atg5*, sense 5'-AAG CAA CTC TGG ATG GGA TT-3' and antisense 5'-GCA GCC ACA GGA CGA AAC-3' (173 bp); β-*actin*, sense 5'-CAC GAT GGA GGG GCC GGA CTC ATC-3' and antisense 5'-TAA AGA CCT CTA TGC CAA CAC AGT-3' (512 bp). PCR was performed with rTaq (TaKaRa, R001A) in a DNA thermal cycler (Maxygen, THERM-1000) according to a standard protocol as follows: 1 cycle of 95°C for 3 min; 30 cycles of 94°C for 45 sec, annealing for 45 sec (50°C for *beclin 1*, 52°C for *atg7* and 56°C for *atg5* and β-*actin*), and 72°C for 1 min; a final extension at 72°C for 10 min; and holding at 4°C. The amount of cDNA used for each PCR was 20 ng in a 25 μl reaction volume. The PCR products (5 μl) were analyzed by electrophoresis through 1% agarose gels and visualized by SYBR Gold (Molecular Probes, S11494) staining.

RNA interference. *Atg5*, *beclin 1* and negative control siRNA were synthesized by Genephama. The sequences of siRNA were as follows: human *atg5* siRNA, sense 5'-GAC GUU GGU AAC UGA CAA ATT-3' and antisense 5'-UUU GUC AGU UAC CAA CGU CTT-3'; human *beclin 1* siRNA, sense 5'-GGA GCC AUU UAU UGA AAC UTT-3' and antisense 5'-GU UUC AAU AAA UGG CUC CTT-3'. The siRNA were transfected with Lipofectamine 2000 reagent (Invitrogen, 11668027) for 48 h in AGS and MKN28 cells according to the manufacturer's protocol.

Co-immunoprecipitation. Cells were treated with or without quercetin for 48 h. Proteins were extracted using lysis buffer (20 mM Tris (pH = 8), 137 mM NaCl, 10% glycerol, 1% NP-40 and 2 mM EDTA). Protein samples were immunoprecipitated with 1 μg of Beclin 1, Bcl-2 or Bcl-x_L antibodies or irrelevant IgG at 4°C under agitation overnight, and the immunoprecipitated protein was pulled down with protein A-agarose beads (Santa cruz, sc-2001) at 4°C under rotary agitation for 4 h. The last supernatant was removed and proteins were eluted by boiling in 2x SDS loading buffer before SDS-PAGE electrophoresis.

Immunohistochemistry. Immunohistochemistry was performed using the Dako EnVision Systems (Dako Cytomation GmbH, Hamburg, Germany). Consecutive paraffin wax-embedded tissue sections (3–5 μm) were dewaxed and rehydrated. Antigen retrieval was performed by pretreatment of the slides in citrate buffer (pH 6.0) in a microwave oven for 12 min. Thereafter slides were cooled to room temperature in deionized water. Endogenous peroxidase activity was quenched by incubating the slides in methanol containing 3% hydrogen peroxide followed by washing in PBS for 5 min after which the sections were incubated for 1 h at room temperature with normal goat serum and subsequently incubated at 4°C overnight with the

primary antibodies. Next the sections were rinsed with washing buffer (PBS with 0.1% bovine serum albumin) and incubated with horseradish peroxidase-linked goat anti-rabbit antibodies followed by reaction with diaminobenzidine and counterstaining with Mayer's hematoxylin.

Tumor xenograft model. The Institutional Animal Care and Treatment Committee of Sichuan University approved all studies herein. Healthy female nude mice (BALB/c, 6–8 weeks of age, nonfertile and 18–20 g each) were injected subcutaneously with MKN28 cells (5 x 10^6 cells/mouse). Once the tumors reached a measurable size (tumor diameter was about 5 mm), animals were randomized into a control group (daily intraperitoneal injection of vehicle: 6% DMSO, 50% PEG-400 in PBS) and a quercetin group (daily intraperitoneal injection of 50 mg/kg quercetin). The tumor volumes were evaluated according to the following formula: tumor volume (mm^3) = (length x $width^2$)/2. Animals were sacrificed 24 d after injection. Tumors were dissected and frozen in liquid nitrogen or fixed in formalin immediately.

Statistical analysis. All quantitative data were presented as the mean ± standard deviation (±SD). Significance of the differences was determined by Student's t test. Statistical significance was defined as $p < 0.05$.

Disclosure of Potential Conflicts of Interest

No potential conflicts of interest were disclosed.

Acknowledgements

This work was supported by grants from the National 973 Basic Research Program of China (2011CB910703), the National 863 High Tech Foundation (2007AA021205), (2008ZX10002-009) and Chinese NSFC (81072022).

Note

Supplemental materials can be found at:
www.landesbioscience.com/journals/autophagy/article/15863

References

1. Liu R, Li Z, Bai S, Zhang H, Tang M, Lei Y, et al. Mechanism of cancer cell adaptation to metabolic stress: proteomics identification of a novel thyroid hormone-mediated gastric carcinogenic signaling pathway. Mol Cell Proteomics 2009; 8:70-85; PMID:18723843; http://dx.doi.org/10.1074/mcp.M800195-MCP200.
2. Ohtsu A. Chemotherapy for metastatic gastric cancer: past, present and future. J Gastroenterol 2008; 43:256-64; PMID:18458840; http://dx.doi.org/10.1007/s00535-008-2177-6.
3. Boots AW, Haenen GR, Bast A. Health effects of quercetin: from antioxidant to nutraceutical. Eur J Pharmacol 2008; 585:325-37; PMID:18417116; http://dx.doi.org/10.1016/j.ejphar.2008.03.008.
4. Baowen Q, Yulin Z, Xin W, Wenjing X, Hao Z, Zhizhi C, et al. A further investigation concerning correlation between anti-fibrotic effect of liposomal quercetin and inflammatory cytokines in pulmonary fibrosis. Eur J Pharmacol 2010; 642:134-9; PMID:20510684; http://dx.doi.org/10.1016/j.ejphar.2010.05.019.
5. Ferry DR, Smith A, Malkhandi J, Fyfe DW, deTakats PG, Anderson D, et al. Phase I clinical trial of the flavonoid quercetin: pharmacokinetics and evidence for in vivo tyrosine kinase inhibition. Clin Cancer Res 1996; 2:659-68; PMID:9816216.
6. Wei YQ, Zhao X, Kariya Y, Fukata H, Teshigawara K, Uchida A. Induction of apoptosis by quercetin: involvement of heat shock protein. Cancer Res 1994; 54:4952-7; PMID:8069862.
7. Murakami A, Ashida H, Terao J. Multitargeted cancer prevention by quercetin. Cancer Lett 2008; 269:315-25; PMID:18467024; http://dx.doi.org/10.1016/j.canlet.2008.03.046.
8. Zhou J, Liang S, Fang L, Chen L, Tang M, Xu Y, et al. Quantitative proteomic analysis of HepG2 cells treated with quercetin suggests IQGAP1 involved in quercetin-induced regulation of cell proliferation and migration. OMICS 2009; 13:93-103; PMID:19207037; http://dx.doi.org/10.1089/omi.2008.0075.
9. Yoshida M, Sakai T, Hosokawa N, Marui N, Matsumoto K, Fujioka A, et al. The effect of quercetin on cell cycle progression and growth of human gastric cancer cells. FEBS Lett 1990; 260:10-3; PMID:2298289; http://dx.doi.org/10.1016/0014-5793(90)80053-L.
10. Eisenberg-Lerner A, Bialik S, Simon HU, Kimchi A. Life and death partners: apoptosis, autophagy and the cross-talk between them. Cell Death Differ 2009; 16:966-75; PMID:19325568; http://dx.doi.org/10.1038/cdd.2009.33.
11. Maiuri MC, Zalckvar E, Kimchi A, Kroemer G. Self-eating and self-killing: crosstalk between autophagy and apoptosis. Nat Rev Mol Cell Biol 2007; 8:741-52; PMID:17717517; http://dx.doi.org/10.1038/nrm2239.
12. Yang Z, Klionsky DJ. Eaten alive: a history of macroautophagy. Nat Cell Biol 2010; 12:814-22; PMID:20811353; http://dx.doi.org/10.1038/ncb0910-814.
13. Shintani T, Klionsky DJ. Autophagy in health and disease: a double-edged sword. Science 2004; 306:990-5; PMID:15528435; http://dx.doi.org/10.1126/science.1099993.
14. Klionsky DJ. The autophagy connection. Dev Cell 2010; 19:11-2; PMID:20643346; http://dx.doi.org/10.1016/j.devcel.2010.07.005.
15. Xie Z, Klionsky DJ. Autophagosome formation: core machinery and adaptations. Nat Cell Biol 2007; 9:1102-9; PMID:17909521; http://dx.doi.org/10.1038/ncb1007-102.
16. Geng J, Klionsky DJ. The Atg8 and Atg12 ubiquitin-like conjugation systems in macroautophagy. 'Protein modifications: beyond the usual suspects' review series. EMBO Rep 2008; 9:859-64; PMID:18704115; http://dx.doi.org/10.1038/embor.2008.163.
17. Kroemer G, Mariño G, Levine B. Autophagy and the integrated stress response. Mol Cell 2010; 40:280-93; PMID:20965422; http://dx.doi.org/10.1016/j.molcel.2010.09.023.
18. Yang Z, Klionsky DJ. Mammalian autophagy: core molecular machinery and signaling regulation. Curr Opin Cell Biol 2010; 22:124-31; PMID:20034776; http://dx.doi.org/10.1016/j.ceb.2009.11.014.
19. Zhang H, Bosch-Marce M, Shimoda LA, Tan YS, Baek JH, Wesley JB, et al. Mitochondrial autophagy is an HIF-1-dependent adaptive metabolic response to hypoxia. J Biol Chem 2008; 283:10892-903; PMID:18281291; http://dx.doi.org/10.1074/jbc.M800102200.
20. Bellot G, Garcia-Medina R, Gounon P, Chiche J, Roux D, Pouysségur J, et al. Hypoxia-induced autophagy is mediated through hypoxia-inducible factor induction of BNIP3 and BNIP3L via their BH3 domains. Mol Cell Biol 2009; 29:2570-81; PMID:19273585; http://dx.doi.org/10.1128/MCB.00166-09.
21. Luo S, Rubinsztein DC. Atg5 and Bcl-2 provide novel insights into the interplay between apoptosis and autophagy. Cell Death Differ 2007; 14:1247-50; PMID:17431417; http://dx.doi.org/10.1038/sj.cdd.4402149.
22. Yousefi S, Perozzo R, Schmid I, Ziemiecki A, Schaffner T, Scapozza L, et al. Calpain-mediated cleavage of Atg5 switches autophagy to apoptosis. Nat Cell Biol 2006; 8:1124-32; PMID:16998475; http://dx.doi.org/10.1038/ncb1482.
23. Levine B, Sinha S, Kroemer G. Bcl-2 family members: dual regulators of apoptosis and autophagy. Autophagy 2008; 4:600-6; PMID:18497563.
24. Paglin S, Hollister T, Delohery T, Hackett N, McMahill M, Sphicas E, et al. A novel response of cancer cells to radiation involves autophagy and formation of acidic vesicles. Cancer Res 2001; 61:439-44; PMID:11212227.
25. Kabeya Y, Mizushima N, Ueno T, Yamamoto A, Kirisako T, Noda T, et al. LC3, a mammalian homologue of yeast Apg8p, is localized in autophagosome membranes after processing. EMBO J 2000; 19:5720-8; PMID:11060023; http://dx.doi.org/10.1093/emboj/19.21.5720.
26. Rubinsztein DC, Cuervo AM, Ravikumar B, Sarkar S, Korolchuk V, Kaushik S, et al. In search of an "autophagomometer". Autophagy 2009; 5:585-9; PMID:19411822; http://dx.doi.org/10.4161/auto.5.5.8823.
27. Tanida I, Ueno T, Kominami E. LC3 conjugation system in mammalian autophagy. Int J Biochem Cell Biol 2004; 36:2503-18; PMID:15325588; http://dx.doi.org/10.1016/j.biocel.2004.05.009.
28. Klionsky DJ, Abeliovich H, Agostinis P, Agrawal DK, Aliev G, Askew DS, et al. Guidelines for the use and interpretation of assays for monitoring autophagy in higher eukaryotes. Autophagy 2008; 4:151-75; PMID:18188003.
29. Yang Z, Klionsky DJ. An overview of the molecular mechanism of autophagy. Curr Top Microbiol Immunol 2009; 335:1-32; PMID:19802558; http://dx.doi.org/10.1007/978-3-642-00302-8_1.
30. Yu L, Alva A, Su H, Dutt P, Freundt E, Welsh S, et al. Regulation of an ATG7-Beclin 1 program of autophagic cell death by caspase-8. Science 2004; 304:1500-2; PMID:15131264; http://dx.doi.org/10.1126/science.1096645.
31. Li J, Liu R, Lei Y, Wang K, Lau QC, Xie N, et al. Proteomic analysis revealed association of aberrant ROS signaling with suberoylanilide hydroxamic acid-induced autophagy in Jurkat T-leukemia cells. Autophagy 2010; 6:711-24; PMID:20543569; http://dx.doi.org/10.4161/auto.6.6.12397.

32. Kim RH, Coates JM, Bowles TL, McNerney GP, Sutcliffe J, Jung JU, et al. Arginine deiminase as a novel therapy for prostate cancer induces autophagy and caspase-independent apoptosis. Cancer Res 2009; 69:700-8; PMID:19147587; http://dx.doi.org/10.1158/0008-5472.CAN-08-3157.
33. Sy LK, Yan SC, Lok CN, Man RY, Che CM. Timosaponin A-III induces autophagy preceding mitochondria-mediated apoptosis in HeLa cancer cells. Cancer Res 2008; 68:10229-37; PMID:19074891; http://dx.doi.org/10.1158/0008-5472.CAN-08-1983.
34. Herman-Antosiewicz A, Johnson DE, Singh SV. Sulforaphane causes autophagy to inhibit release of cytochrome *C* and apoptosis in human prostate cancer cells. Cancer Res 2006; 66:5828-35; PMID:16740722; http://dx.doi.org/10.1158/0008-5472.CAN-06-0139.
35. Fimia GM, Piacentini M. Regulation of autophagy in mammals and its interplay with apoptosis. Cell Mol Life Sci 2010; 67:1581-8; PMID:20165902; http://dx.doi.org/10.1007/s00018-010-0284-z.
36. Yorimitsu T, Klionsky DJ. Autophagy: molecular machinery for self-eating. Cell Death Differ 2005; 12:1542-52; PMID:16247502; http://dx.doi.org/10.1038/sj.cdd.4401765.
37. Pouysségur J, Dayan F, Mazure NM. Hypoxia signalling in cancer and approaches to enforce tumour regression. Nature 2006; 441:437-43; PMID:16724055; http://dx.doi.org/10.1038/nature04871.
38. Jeong JH, An JY, Kwon YT, Rhee JG, Lee YJ. Effects of low dose quercetin: cancer cell-specific inhibition of cell cycle progression. J Cell Biochem 2009; 106:73-82; PMID:19009557; http://dx.doi.org/10.1002/jcb.21977.
39. Pattingre S, Tassa A, Qu X, Garuti R, Liang XH, Mizushima N, et al. Bcl-2 antiapoptotic proteins inhibit Beclin 1-dependent autophagy. Cell 2005; 122:927-39; PMID:16179260; http://dx.doi.org/10.1016/j.cell.2005.07.002.
40. Yang Z, Klionsky DJ. An overview of the molecular mechanism of autophagy. Curr Top Microbiol Immunol 2009; 335:1-32; PMID:19802558; http://dx.doi.org/10.1007/978-3-642-00302-8_1.
41. Ogata A, Yanagie H, Ishikawa E, Morishita Y, Mitsui S, Yamashita A, et al. Antitumour effect of polyoxomolybdates: induction of apoptotic cell death and autophagy in in vitro and in vivo models. Br J Cancer 2008; 98:399-409; PMID:18087283; http://dx.doi.org/10.1038/sj.bjc.6604133.
42. Chen YJ, Huang WP, Yang YC, Lin CP, Chen SH, Hsu ML, et al. Platonin induces autophagy-associated cell death in human leukemia cells. Autophagy 2009; 5:173-83; PMID:19066447; http://dx.doi.org/10.4161/auto.5.2.7360.
43. Bommareddy A, Hahm ER, Xiao D, Powolny AA, Fisher AL, Jiang Y, et al. Atg5 regulates phenethyl isothiocyanate-induced autophagic and apoptotic cell death in human prostate cancer cells. Cancer Res 2009; 69:3704-12; PMID:19336571; http://dx.doi.org/10.1158/0008-5472.CAN-08-4344.
44. Sun ZJ, Chen G, Hu X, Zhang W, Liu Y, Zhu LX, et al. Activation of PI3K/Akt/IKK-alpha/NFkappaB signaling pathway is required for the apoptosis-evasion in human salivary adenoid cystic carcinoma: its inhibition by quercetin. Apoptosis 2010; 15:850-63; PMID:20386985; http://dx.doi.org/10.1007/s10495-010-0497-5.
45. Kim YH, Lee YJ. TRAIL apoptosis is enhanced by quercetin through Akt dephosphorylation. J Cell Biochem 2007; 100:998-1009; PMID:17031854; http://dx.doi.org/10.1002/jcb.21098.
46. Semenza GL. Targeting HIF-1 for cancer therapy. Nat Rev Cancer 2003; 3:721-32; PMID:13130303; http://dx.doi.org/10.1038/nrc1187.
47. Denko NC. Hypoxia, HIF1 and glucose metabolism in the solid tumour. Nat Rev Cancer 2008; 8:705-13; PMID:19143055; http://dx.doi.org/10.1038/nrc2468.
48. Radreau P, Rhodes JD, Mithen RF, Kroon PA, Sanderson J. Hypoxia-inducible factor-1 (HIF-1) pathway activation by quercetin in human lens epithelial cells. Exp Eye Res 2009; 89:995-1002; PMID:19729006; http://dx.doi.org/10.1016/j.exer.2009.08.011.
49. Park SS, Bae I, Lee YJ. Flavonoids-induced accumulation of hypoxia-inducible factor (HIF)-1alpha/2alpha is mediated through chelation of iron. J Cell Biochem 2008; 103:1989-98; PMID:17973296; http://dx.doi.org/10.1002/jcb.21588.
50. Triantafyllou A, Liakos P, Tsakalof A, Chachami G, Paraskeva E, Molyvdas PA, et al. The flavonoid quercetin induces hypoxia-inducible factor-1alpha (HIF-1alpha) and inhibits cell proliferation by depleting intracellular iron. Free Radic Res 2007; 41:342-56; PMID:17364964; http://dx.doi.org/10.1080/10715760601055324.
51. Leopoldini M, Russo N, Chiodo S, Toscano M. Iron chelation by the powerful antioxidant flavonoid quercetin. J Agric Food Chem 2006; 54:6343-51; PMID:16910729; http://dx.doi.org/10.1021/jf060986 h.
52. Lu HH, Kao SY, Liu TY, Liu ST, Huang WP, Chang KW, et al. Areca nut extract induced oxidative stress and upregulated hypoxia inducing factor leading to autophagy in oral cancer cells. Autophagy 2010; 6:725-37; PMID:20523123; http://dx.doi.org/10.4161/auto.6.6.12423.
53. Zhang H, Bosch-Marce M, Shimoda LA, Tan YS, Baek JH, Wesley JB, et al. Mitochondrial autophagy is an HIF-1-dependent adaptive metabolic response to hypoxia. J Biol Chem 2008; 283:10892-903; PMID:18281291; http://dx.doi.org/10.1074/jbc.M800102200.
54. Yamamura Y, Lee WL, Inoue K, Ida H, Ito Y. RUNX3 cooperates with FoxO3a to induce apoptosis in gastric cancer cells. J Biol Chem 2006; 281:5267-76; PMID:16373335; http://dx.doi.org/10.1074/jbc.M512151200.
55. Espert L, Denizot M, Grimaldi M, Robert-Hebmann V, Gay B, Varbanov M, et al. Autophagy is involved in T cell death after binding of HIV-1 envelope proteins to CXCR4. J Clin Invest 2006; 116:2161-72; PMID:16886061; http://dx.doi.org/10.1172/JCI26185.
56. Paglin S, Lee NY, Nakar C, Fitzgerald M, Plotkin J, Deuel B, et al. Rapamycin-sensitive pathway regulates mitochondrial membrane potential, autophagy, and survival in irradiated MCF-7 cells. Cancer Res 2005; 65:11061-70; PMID:16322256; http://dx.doi.org/10.1158/0008-5472.CAN-05-1083.